Available online at www.sciencedirect.com
SCIENCE DIRECT®
Nuclear Physics B 709 (2005) 419–439
NUCLEAR PHYSICS B

Constraints on scalar couplings from $\pi^{\pm} \to l^{\pm}\nu_l$

Bruce A. Campbell, David W. Maybury

Department of Physics, University of Alberta, Edmonton AB T6G 2J1, Canada

Received 1 June 2004; accepted 14 December 2004

Available online 30 December 2004

Abstract

New interactions with Lorentz scalar structure, arising from physics beyond the standard model of electroweak interactions, will induce effective pseudoscalar interactions after renormalization by weak interaction loop corrections. Such induced pseudoscalar interactions are strongly constrained by data on $\pi^{\pm} \to l^{\pm}\nu_l$ decay. These limits on induced pseudoscalar interactions imply limits on the underlying fundamental scalar interactions that in many cases are substantially stronger than limits on scalar interactions from direct β-decay searches.
© 2004 Elsevier B.V. All rights reserved.

PACS: 12.15.Lk; 12.90.+b; 13.20.Cz; 14.40.Cs

1. Introduction

While there is strong support for the $V - A$ form of the charged weak current, it is possible that new physics at or above the weak scale could give rise to scalar interactions that would compete with standard model processes. Examples of such possible physics include the exchange of extra Higgs multiplets which could enter the theory at scales from the Z mass upwards [1], leptoquarks which could be present at scales above 200 GeV [1], contact interactions from quark/lepton compositeness which could be present at the TeV scale [1], or strong gravitational interactions in TeV brane world models [1]. Recently, precision experiments [2–4] have searched for scalar interactions in β-decay, however, direct

E-mail address: dmaybury@phys.ualberta.ca (D.W. Maybury).

0550-3213/$ – see front matter © 2004 Elsevier B.V. All rights reserved.
doi:10.1016/j.nuclphysb.2004.12.015

experimental constraints on scalar couplings still remain relatively weak as compared to the corresponding limits on pseudoscalar couplings [1,5].

The precision of the limits on pseudoscalar couplings comes in part from the fact that the pion, a pseudoscalar meson, has a chirally suppressed decay $\pi^{\pm} \to l^{\pm}\nu_l$ which would be sensitive to new pseudoscalar interactions [6]. These pseudoscalar interactions would be detected by the failure of the standard model prediction [7] for the chiral suppression in the ratio of branching ratios $\frac{\Gamma(\pi^- \to e\bar{\nu})}{\Gamma(\pi^- \to \mu\bar{\nu})}$. It is the large chiral suppression factor, by the square of the electron–muon mass ratio, that allows such a powerful test of new physics that violates chirality and parity.

In the standard model, the leading contribution to pion decay occurs through tree level W exchange. At the quark level, this is the same process that is involved in the β-decay of a nucleon ignoring the spectator quarks. While the pion cannot decay through a scalar interaction, the pion can decay through induced pseudoscalar interactions generated from the electroweak renormalization of the scalar couplings. It is of considerable interest to use limits on the induced pseudoscalar couplings to set indirect limits on the size of the underlying scalar interactions.

In the following sections we outline our methods and estimate the limits on the size of scalar couplings based on the indirect effects from charged pion decay. We use general operator techniques to obtain model independent results and we combine these results with data from pion decay and also muon capture, to constrain the scalar couplings indirectly. We also discuss some of the implications of these results and comment on prospects for future searches for scalar interactions.

2. Pion physics and new pseudoscalar interactions

Consider constructing an effective Lagrangian and matrix element for the process $\pi^{\pm} \to l^{\pm}\nu_l$ in the presence of pseudoscalar interactions. We can set limits on the strength of the pseudoscalar interactions from their interference with tree level W exchange. Since the pion is a pseudoscalar, we can use the following relations for current matrix elements:

$$\begin{aligned}
&\langle 0|\bar{u}\gamma_\mu\gamma_5 d\big|\pi(p)\big\rangle = i\sqrt{2} f_\pi p_\mu,\\
&\langle 0|\bar{u}\gamma_5 d\big|\pi(p)\big\rangle = i\sqrt{2}\tilde{f}_\pi = i\sqrt{2}\frac{f_\pi m_\pi^2}{m_u + m_d},\\
&\langle 0|\bar{u}\sigma^{\mu\nu}\gamma_5 d\big|\pi(p)\big\rangle = 0,\\
&\langle 0|\bar{u}\sigma^{\mu\nu} d\big|\pi(p)\big\rangle = 0,
\end{aligned} \tag{1}$$

where $f_\pi = 93$ MeV and $\tilde{f}_\pi = 1.8 \times 10^5$ MeV^2. The matrix element for the tree level W contribution can easily be constructed by using Eq. (1), giving

$$\mathcal{M}_{W^{\pm}} = G_F f_\pi \cos\theta_c \big[\bar{l}\gamma^\mu(1-\gamma_5)\nu_l\big] p_\mu, \tag{2}$$

where p_μ is the pion momentum and θ_c is the Cabibbo angle. A pseudoscalar contribution with left-handed neutrinos in the final state can be expressed as a four-Fermi contact

operator,

$$\mathcal{L}_P = -i\frac{\rho}{2\Lambda^2}\big[\bar{l}(1-\gamma_5)\nu_l\big][\bar{u}\gamma_5 d], \tag{3}$$

where ρ is the pseudoscalar coupling constant. This expression can be converted to a matrix element using Eq. (1)

$$\mathcal{M}_P = \rho\frac{\tilde{f}_\pi}{\sqrt{2}\Lambda^2}\big[\bar{l}(1-\gamma_5)\nu_l\big]. \tag{4}$$

In the presence of a pseudoscalar interaction, the overall matrix element for the process $\pi^\pm \to l^\pm \nu_l$ is the coherent sum, $\mathcal{M}_P + \mathcal{M}_{W^\pm} = \mathcal{M}_l$,

$$\mathcal{M}_l = G_F f_\pi \cos\theta_c\big[\bar{l}\gamma^\mu(1-\gamma_5)\nu_l\big]p_\mu + \frac{\rho\tilde{f}_\pi}{\sqrt{2}\Lambda^2}\big[\bar{l}(1-\gamma_5)\nu_l\big]. \tag{5}$$

Having constructed the matrix element, we can now estimate the ratio of branching ratios

$$\frac{\Gamma(\pi^-\to e\nu_e)}{\Gamma(\pi^-\to\mu\nu_\mu)} = \frac{(m_\pi^2-m_e^2)}{(m_\pi^2-m_\mu^2)}\frac{\langle|M_{ev}|^2\rangle}{\langle|M_{\mu\nu}|^2\rangle}. \tag{6}$$

Summing over final states of the squared matrix element we have

$$\begin{aligned}\big\langle|\mathcal{M}_l|^2\big\rangle &= 4G_f^2 f_\pi^2\cos^2\theta_c m_l^2\big(m_\pi^2-m_l^2\big) + 8\frac{G_F\tilde{f}_\pi f_\pi\cos\theta_c\rho}{\sqrt{2}\Lambda^2}m_l\big(m_\pi^2-m_l^2\big)\\ &\quad + 2\frac{\rho^2\tilde{f}_\pi^2}{\Lambda^4}\big(m_\pi^2-m_l^2\big).\end{aligned} \tag{7}$$

For simplicity we have assumed that the pseudoscalar coupling is real, however, in general ρ may be complex. The more general expression is obtained by making the following replacements:

$$\begin{aligned}&\rho\to\frac{\rho+\rho^*}{2} = \mathrm{Re}(\rho),\\ &(\rho)^2\to|\rho|^2.\end{aligned} \tag{8}$$

We find that the branching ratio is given by

$$\frac{\Gamma(\pi^-\to e\nu_e)}{\Gamma(\pi^-\to\mu\nu_\mu)} = \frac{(m_\pi^2-m_e^2)}{(m_\pi^2-m_\mu^2)}\left[\frac{m_e^2(m_\pi^2-m_e^2)+R_e}{m_\mu^2(m_\pi^2-m_\mu^2)+R_\mu}\right], \tag{9}$$

where the $R_{e,\mu}$ functions are

$$\begin{aligned}R_{e,\mu} &= \sqrt{2}\frac{\tilde{f}_\pi\,\mathrm{Re}(\rho)}{G_F f_\pi\Lambda^2\cos\theta_c}m_{e,\mu}\big(m_\pi^2-m_{e,\mu}^2\big)\\ &\quad + \frac{|\rho|^2\tilde{f}_\pi^2}{2f_\pi^2G_F^2\Lambda^4\cos^2\theta_c}\big(m_\pi^2-m_{e,\mu}^2\big).\end{aligned} \tag{10}$$

Thus far we have only discussed interactions with left-handed neutrinos in the final state. The inclusion of right-handed neutrinos requires a modification since pseudoscalar

contributions to decays with right-handed neutrinos in the final state cannot interfere with the W exchange graph; hence the contributions to the rate add incoherently. With right-handed neutrinos, the expression for the matrix element becomes

$$\mathcal{M}_P = \frac{\rho' \tilde{f}_\pi}{\sqrt{2}\Lambda^2}\big[\bar{l}(1+\gamma_5)\nu_l\big], \tag{11}$$

where ρ' is the pseudoscalar coupling involving right-handed neutrinos. Defining

$$T \equiv \frac{(m_\pi^2 - m_e^2)^2}{(m_\pi^2 - m_\mu^2)^2}\frac{m_e^2}{m_\mu^2} = 1.28 \times 10^{-4}, \tag{12}$$

we can express the branching ratio as

$$\begin{aligned}\frac{\Gamma(\pi^- \to e\nu_e)}{\Gamma(\pi^- \to \mu\nu_\mu)} &= T\left(\frac{1 + \sqrt{2}\frac{\tilde{f}_\pi \operatorname{Re}(\rho_e)}{G_F\Lambda^2 f_\pi \cos\theta_c m_e} + \frac{|\rho_e|^2\tilde{f}_\pi^2}{2G_F^2\Lambda^4 f_\pi^2\cos^2\theta_c m_e^2} + \frac{|\rho'_e|^2\tilde{f}_\pi^2}{2G_F^2 f_\pi^2\Lambda^4\cos^2\theta_c m_e^2}}{1 + \sqrt{2}\frac{\tilde{f}_\pi \operatorname{Re}(\rho_\mu)}{G_F\Lambda^2 f_\pi \cos\theta_c m_\mu} + \frac{|\rho_\mu|^2\tilde{f}_\pi^2}{2G_F^2\Lambda^4 f_\pi^2\cos^2\theta_c m_\mu^2} + \frac{|\rho'_\mu|^2\tilde{f}_\pi^2}{2G_F^2\Lambda^4 f_\pi^2\cos^2\theta_c m_\mu^2}}\right).\end{aligned} \tag{13}$$

If we assume either universal scalar couplings or else scalar couplings involving only the first generation, we obtain the following approximation for the ratio of decay widths:

$$\begin{aligned}\frac{\Gamma(\pi^- \to e\nu_e)}{\Gamma(\pi^- \to \mu\nu_\mu)} &\approx T\left(1 + \sqrt{2}\frac{\tilde{f}_\pi \operatorname{Re}(\rho)}{G_F\Lambda^2 f_\pi \cos\theta_c m_e} + \frac{|\rho|^2\tilde{f}_\pi^2}{2G_F^2\Lambda^4 f_\pi^2\cos^2\theta_c m_e^2}\right.\\ &\quad\left. + \frac{|\rho'|^2\tilde{f}_\pi^2}{2G_F^2\Lambda^4 f_\pi^2\cos^2\theta_c m_e^2}\right).\end{aligned} \tag{14}$$

We will discuss the effects of more general generation dependence of the scalar couplings in Section 6. The theoretical standard model calculation including radiative corrections is $\mathrm{Br}_{\mathrm{th}} = (1.2352 \pm 0.0005) \times 10^{-4}$ [7] and the measured experimental branching ratio is $\mathrm{Br}_{\mathrm{exp}} = (1.230 \pm 0.0040) \times 10^{-4}$ [1,8–10]. Combining the experimental and theoretical uncertainties in quadrature, we can obtain a bound on the pseudoscalar couplings at 2σ,

$$\begin{aligned}&-1.0 \times 10^{-2}\\ &\quad\leqslant \sqrt{2}\frac{\tilde{f}_\pi \operatorname{Re}(\rho)}{G_F\Lambda^2 f_\pi \cos\theta_c m_e} + \frac{|\rho|^2\tilde{f}_\pi^2}{2G_F^2\Lambda^4 f_\pi^2\cos^2\theta_c m_e^2} + \frac{|\rho'|^2\tilde{f}_\pi^2}{2G_F^2\Lambda^4 f_\pi^2\cos^2\theta_c m_e^2}\\ &\quad\leqslant 2.2 \times 10^{-3}.\end{aligned} \tag{15}$$

3. Local scalar operator analysis

Electroweak interactions can radiatively induce pseudoscalar operators from pure scalar interactions. Suppose that at some scale Λ there exists new physics that generates a purely

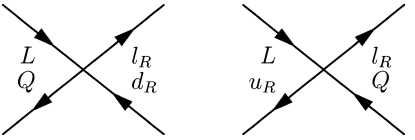

Fig. 1. $\mathcal{O}_1$ and $\mathcal{O}_2$, type A contact interactions.

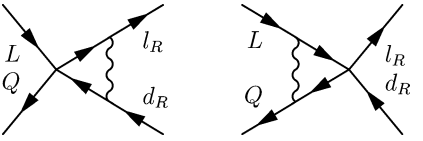

Fig. 2. Example of electroweak corrections to type A contact interactions. All permutations are required including wavefunction renormalization; the vector bosons are the $W_\mu^{1,2,3}$ and B_μ.

scalar four-Fermi interaction. It may be due to the exchange of fundamental scalars or it may be due to a variety of other physics such as compositeness, extra dimensions, lepto-quarks, et cetera. Independent of the details of the new physics that generates the scalar interactions, they will appear as non-renormalizable four-Fermi scalar contact operators below the scale Λ.

In order to facilitate power counting, the $\overline{\text{MS}}$ scheme is most often used with effective field theory [11]. The $\overline{\text{MS}}$ scheme (or any mass independent subtraction scheme) presents the subtlety that heavy particles do not decouple in beta function calculations. That is, mass independent renormalization schemes do not satisfy the conditions of the Applequist–Carazzone theorem [11]. This is dealt with by simply integrating out the heavy fields by hand at their associated scale. Thus whether we analyze the effective interactions in a UV complete theory or in the effective theory, we will arrive at the same renormalization group running (up to threshold corrections) provided that we are only interested in results below Λ and only up to some finite power of $(\frac{1}{\Lambda})$.

We start by considering SU(2) × U(1) invariant four-fermion contact interactions that are generation independent and flavour diagonal (see Figs. 1 and 4). We will discuss the effects of generation dependence in Section 6. We consider two types of scalar operators in order to facilitate comparison with the direct experimental constraints. Type A (O_A) have left-handed neutrinos in the final state while type B (O_B) have right-handed (sterile) neutrinos. These interactions appear as extensions to the standard model Lagrangian involving non-renormalizable operators,

$$\mathcal{L}_{\text{scalar}} = \frac{s_A}{\Lambda^2} O_A + \frac{s_B}{\Lambda^2} O_B, \tag{16}$$

where s_A and s_B are undetermined scalar couplings. From these interactions, electroweak radiative corrections (see Figs. 2 and 5) can in principle induce pseudoscalar interactions. We retain corrections up to order $\frac{1}{\Lambda^2}$ and from this analysis we extract the anomalous dimension matrix.

3.1. Type A operator analysis: O_A

The operators of type A are as follows:

$$O_1 = [\bar{e}_R L][\bar{Q} d_R], \tag{17}$$

$$O_2 = [\bar{e}_R L][\bar{u}_R Q] \tag{18}$$

(where the SU(2) indices have been suppressed) such that the pure scalar interaction is

$$O_A = O_1 + O_2. \tag{19}$$

Since we are assuming that at the scale Λ there is a pure scalar interaction, we take O_1 and O_2 to enter the theory at the high scale with equal weight.

In calculating the anomalous dimension matrix a third operator is generated through renormalization: the operator $O' = [\bar{e}_R Q][\bar{u}_R L]$ mixes with the other two. However, in order to construct the matrix element for the pion decay amplitude, we need to rotate the operators to a basis that has a definite matrix element between the vacuum and the on-shell pion state. This requires Fierz reordering

$$O' = -\frac{1}{2} O_2 + \left(-\frac{1}{8}\right)\left[\bar{e}_R \sigma_{\mu\nu} L\right]\left[\bar{u}_R \sigma^{\mu\nu} Q\right], \tag{20}$$

where we define

$$O_3 \equiv \left(-\frac{1}{8}\right)\left[\bar{e}_R \sigma_{\mu\nu} L\right]\left[\bar{u}_R \sigma^{\mu\nu} Q\right]. \tag{21}$$

Note that $\langle 0|O_3|\pi(p)\rangle = 0$. This leaves us with the following beta functions:

$$\mu \frac{\partial(\mathcal{O})}{\partial \mu} = \frac{1}{32\pi^2}\gamma \mathcal{O}, \tag{22}$$

where

$$\mathcal{O} = \begin{pmatrix} O_1 \\ O_2 \\ O_3 \end{pmatrix} \tag{23}$$

and

$$\gamma = \begin{bmatrix} 6g^2 + \frac{98}{9}g'^2 & 0 & 0 \\ 0 & 6g^2 + \frac{128}{9}g'^2 & 6g^2 + 10g'^2 \\ 0 & \frac{9}{2}g^2 + \frac{15}{2}g'^2 & 12g^2 + \frac{103}{9}g'^2 \end{bmatrix}. \tag{24}$$

The constants g' and g are the U(1) and SU(2) coupling constants, respectively. The results of the numerical integration of the renormalization group equations are displayed in Fig. 3. O_1 and O_2 start out with equal amplitude at the scale Λ. They are then renormalized to the weak scale of roughly 100 GeV. In the first panel the x-axis indicates the starting scale Λ, i.e., the scale of new physics. The y-axis indicates the amount each operator is suppressed in running from the scale Λ to the weak scale. Each operator renormalizes differently and the splittings give rise to the pseudoscalar interaction. If the scale Λ is at or very near the weak scale then threshold effects become important, which we will discuss in the following section. The second panel plots the difference of O_1 and O_2 as a function of scale. This difference is proportional to the amount of pseudoscalar interaction induced.

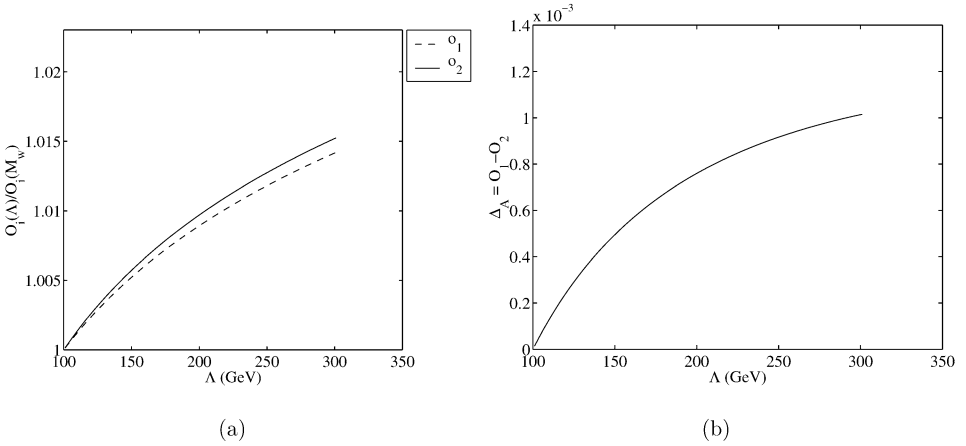

Fig. 3. Type A operator RGE analysis. Panel (a) shows how each operator evolves with scale. Panel (b) displays the induced pseudoscalar proportionality factor.

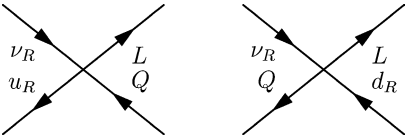

Fig. 4. $\mathcal{O}_1$ and $\mathcal{O}_2$, type B contact interactions.

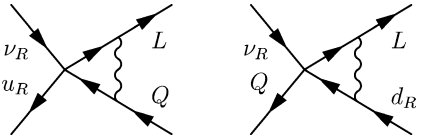

Fig. 5. Example of electroweak corrections to type B contact interactions. All permutations are required including wavefunction renormalization; the vector bosons are the $W_\mu^{1,2,3}$ and B_μ.

3.2. Type B operator analysis: O_B

The type B operators are as follows:

$$O_1 = [\bar{L}\nu_R][\bar{Q}d_R], \tag{25}$$

$$O_2 = [\bar{L}\nu_R][\bar{u}_R Q] \tag{26}$$

(where the SU(2) indices have been suppressed) with

$$O_B = O_1 + O_2. \tag{27}$$

We assume that the interaction at the scale Λ is purely scalar as in the type A scenario. Again operator mixing is present with a third induced operator, namely $O' = [\bar{L}d_R][\bar{Q}\nu_R]$ which must be rotated as before into the appropriate basis: $O' = -\frac{1}{2}O_2 +$

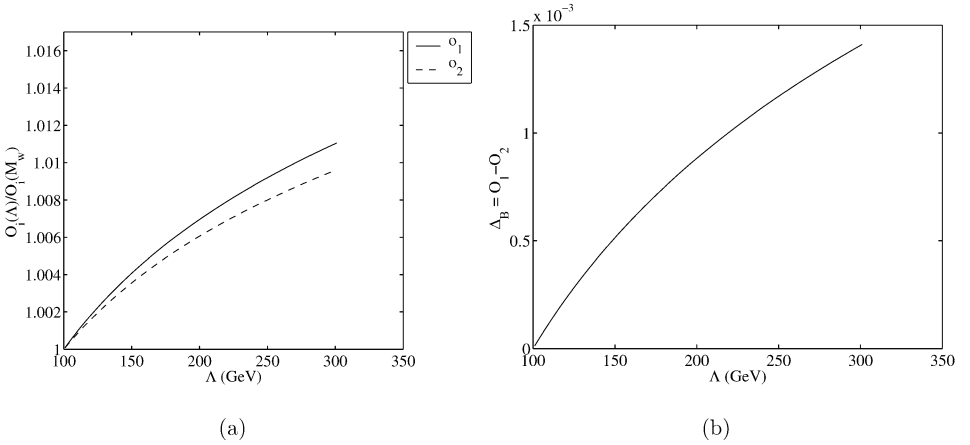

Fig. 6. Type B operator RGE analysis. Panel (a) shows how each operator evolves with scale. Panel (b) displays the induced pseudoscalar proportionality factor.

$(-\frac{1}{8})[\bar{L}\sigma^{\mu\nu}\nu_R][\bar{Q}\sigma_{\mu\nu}d_R]$ where $O_3 = (-\frac{1}{8})[\bar{L}\sigma^{\mu\nu}\nu_R][\bar{Q}\sigma_{\mu\nu}d_R]$. We extract the following anomalous dimension matrix:

$$\mu\frac{\partial(\mathcal{O})}{\partial\mu} = \frac{1}{32\pi^2}\gamma\mathcal{O}, \tag{28}$$

where

$$\mathcal{O} = \begin{pmatrix} O_1 \\ O_2 \\ O_3 \end{pmatrix} \tag{29}$$

and

$$\gamma = \begin{bmatrix} 6g^2 + \frac{38}{9}g'^2 & 0 & 0 \\ 0 & 6g^2 + \frac{11}{9}g'^2 & 6g^2 - \frac{2}{3}g'^2 \\ 0 & \frac{9}{2}g^2 - \frac{1}{3}g'^2 & 12g^2 + \frac{34}{9}g'^2 \end{bmatrix}. \tag{30}$$

The results of the numerical integration of the renormalization group equations are displayed in Fig. 6. As we have seen before in Section 3.1 the graphs in Fig. 6 illustrate the effects of renormalization on the operators O_1 and O_2 when they enter with the same amplitude at the scale Λ.

In both type A and B scalar interactions we see that renormalization effects induce a pseudoscalar interaction. The size of the pseudoscalar interaction depends on how far the scale Λ is from the weak scale. The larger the scale separation is, the larger the induced pseudoscalar proportionality factor becomes. The effective pseudoscalar couplings, which we denoted as ρ and ρ' in Section 2, are given by

$$\begin{aligned} \rho &= s_A\Delta_A(\Lambda), \\ \rho' &= s_B\Delta_B(\Lambda), \end{aligned} \tag{31}$$

where Δ_A and Δ_B are the renormalization group factors induced from the running from the scale Λ down to the weak scale (Δ_A and Δ_B are plotted in the second panel of Figs. 3 and 6). The factors s_A and s_B are the undetermined scalar coupling constants introduced in Eq. (16). Since the pseudoscalar is induced from a scalar interaction we are now in a position to place limits on the magnitude of the scalar coupling from pion physics; the scalar couplings s_A and s_B at the scale of the new physics Λ are now constrained by the requirement that ρ and ρ' satisfy Eq. (15).

A comment on QCD corrections is in order. QCD is a parity invariant theory and therefore QCD corrections cannot induce a pseudoscalar interaction by themselves. In our analysis, the induced pseudoscalar arises from the difference of two operators that initially combined to give a purely scalar interaction and the QCD corrections will affect the two operators in the same way. The QCD corrections can only adjust this difference by an overall multiplicative factor. This is true for both operators of type A and B. However, in Section 5 we compare the direct experimental constraints on scalar couplings from β decay to the indirect constraints on the renormalization induced pseudoscalar interactions from pion decay. Since the same scalar operators are involved in both processes, the QCD effects are the same for each case and therefore will cancel in a comparison of the relative strengths of the limits from the two processes. The largest part of the QCD renormalization of the scalar operators (and hence of their weak interaction induced pseudoscalar difference) will come from the QCD induced running from the weak scale down to the chiral symmetry breaking scale, of order $4\pi f_\pi \approx 1$ GeV [12], where we take the pion decay matrix element using PCAC. The correction to each of the operators can be computed through the QCD renormalization group running of these operators

$$O_{A,B}(1\ \text{GeV}) = \left(\frac{\alpha_s(1\ \text{GeV}^2)}{\alpha_s(M_W^2)}\right)^{4/21} O_{A,B}(M_w) \approx 1.3 O_{A,B}(M_w) \tag{32}$$

for $\Lambda_{\text{QCD}} = 200$ MeV. The induced pseudoscalar, which is proportional to $\Delta_{A,B}$, will be enhanced by this factor of 1.3.

4. Pseudoscalar interactions from threshold effects

A limitation of the renormalization group operator analysis of the last section is its inapplicability if the scale of new physics is at or very near the electroweak scale. In this case, threshold effects become the dominate contribution. To estimate the threshold effects, we consider a toy model where a VEVless scalar doublet is added to the standard model. Indeed it is only for the exchange of a scalar doublet that we need to consider a possible scale for new physics near the electroweak scale. For leptoquarks, compositeness, and extra dimensional gravity, direct experimental constraints imply [1] that the scale Λ of new physics is sufficiently above the electroweak scale that RGE running dominates threshold effects. In principle, the addition of a VEVless scalar doublet can lead to both scalar and pseudoscalar interactions in the tree level Lagrangian. Since pseudoscalar interactions are directly constrained by tree level contributions to pion decay and we are presently interested in limits on pure scalar interactions, we arrange the couplings such that only scalar

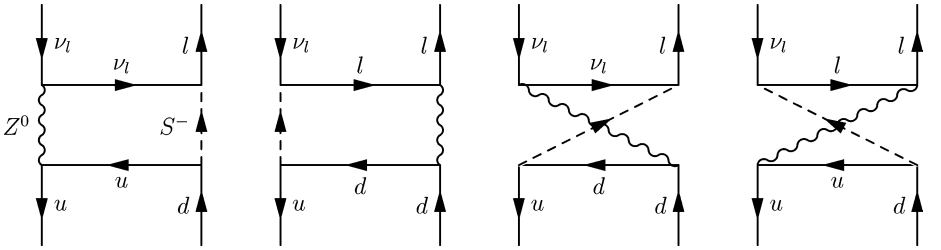

Fig. 7. Dressed Z^0 exchange diagrams.

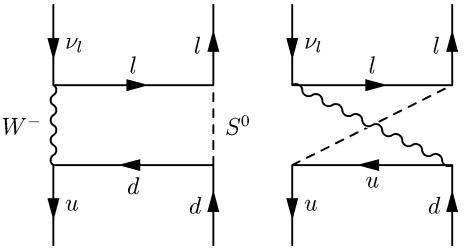

Fig. 8. Dressed W exchange diagrams.

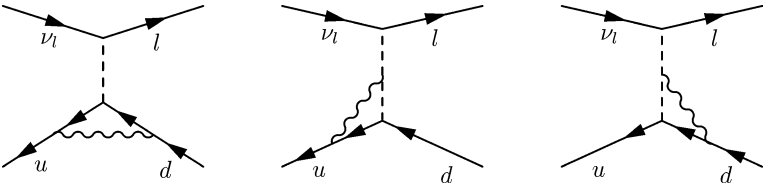

Fig. 9. Radiative corrections to the quark-scalar vertex.

interactions arise at the scale of new physics,

$$\mathcal{L} = (\lambda)\bar{L}e_R S + (\lambda')\bar{Q}d_R S - (\lambda')\bar{Q}u_R\tilde{S} + \text{h.c.}, \tag{33}$$

where λ and λ' are the scalar couplings to the quarks and leptons, respectively, and $\tilde{S} = i\sigma^2 S$. In this working example, the scalar interactions have the property that they couple in a universal and flavour diagonal manner with undetermined scalar couplings to quarks and leptons. It is the charged scalar couplings that the β-decay experiments constrain directly. The pseudoscalar interaction can potentially be induced at one loop through three classes of diagrams: scalar-dressed Z exchange box diagrams, scalar-dressed W exchange box diagrams and radiative corrections to the quark vertex (see Figs. 7–9). The weak interactions do not respect parity and the scalar interactions change chirality, thus diagrams of this form can potentially induce a pseudoscalar interaction. To estimate the effect of the scalar on the branching ratio, we will make the approximation that the quarks are massless and ignore external momenta. Box diagrams that involve the Higgs or the Goldstone modes can be ignored since the couplings are mass proportional and hence their contribution is small.

By explicit calculation we can show that while both the dressed W and Z exchange box diagrams give non-zero amplitudes, their tensor structure is such that after taking the matrix element between the pion and the vacuum they give vanishing contributions. In the vertex correction class of diagrams we are dealing with primitively divergent graphs (see Fig. 9). In order to obtain a conservative estimate of the induced pseudoscalar arising already from threshold effects, we can regulate the loop diagrams by cutting off the loop momentum at the weak scale and integrate from 0 to M_Z. Cutting off the loop momentum at M_Z represents a conservative estimate, in that the scale of new physics is at the weak scale and therefore there is no scale separation for renormalization group running proper. In this case we find a non-vanishing contribution. The three graphs in Fig. 9 give the following result for the pion decay matrix element:

$$\begin{aligned}\mathcal{M}_{\text{Vertex}} &= -\frac{\sqrt{2}g^2\tilde{f}_\pi\lambda\lambda'}{64\pi^2\cos^2\theta_w M_Z^2} \\ &\quad\times\left[\left(-\frac{4}{3}\sin^2\theta_w\right)\ln(2)+\cos(2\theta_w)\left(\ln(2)-\frac{1}{2}\right)\right]\left[\bar{l}(1-\gamma_5)\nu_l\right] \\ &\approx 0.13\frac{\sqrt{2}g^2\tilde{f}_\pi\lambda\lambda'}{64\pi^2\cos^2\theta_w M_Z^2}\left[\bar{l}(1-\gamma_5)\nu_l\right]. \end{aligned} \tag{34}$$

To get a second, independent, estimate of the threshold corrections, in a different renormalization prescription, we will imagine integrating out the weak scale degrees of freedom (W, Z and scalars) to get an effective low-energy theory. The resulting theory will have only dimension six four-fermion operators; to simplify our calculation let us imagine setting the scalar masses just below the mass of the W and Z and integrating out the W and Z first and then immediately integrating out the scalars, thus inducing the four-fermion operators. If we use a dimensionless regulator, the effective fermion-scalar theory after integrating out the W and Z will have Yukawa couplings shifted by threshold effects necessary to reproduce the residual effects of the W and Z in the resulting effective theory in which they are absent. These threshold corrections have been computed in [13,14]. We then immediately integrate out the scalars, with their corrected Yukawa couplings, to get the final low-energy effective theory of fermions with four-fermion couplings. Using the results for the threshold corrections for Yukawa couplings from [13,14], with the gauge charge representations of our particles, and then immediately integrating out the scalars at the weak scale (which we take to be M_Z) we get an effective induced interaction from the vertex corrections of

$$\mathcal{M}_{\text{Vertex}} \approx 0.08\frac{\sqrt{2}g^2\tilde{f}_\pi\lambda\lambda'}{64\pi^2\cos^2\theta_w M_Z^2}\left[\bar{l}(1-\gamma_5)\nu_l\right]. \tag{35}$$

That the estimates of Eqs. (34) and (35), which use two entirely different regularization and renormalization prescriptions, agree to within a factor of two gives us confidence that estimates of the threshold corrections are of this order and are not artifacts of the regulator chosen. To be conservative, we will use the estimate of Eq. (35) which in conjunction with Eq. (15) and in the absence of right-handed neutrinos gives

$$-3\times 10^{-2} \leqslant \frac{K_s}{G_F} \leqslant 6\times 10^{-3}, \tag{36}$$

where

$$|K_s| \equiv \frac{\lambda\lambda'}{M_Z^2}. \tag{37}$$

The above calculation gives a conservative estimate of the amplitude, including only contributions from threshold effects. We see in this toy example that even from threshold effects alone a pseudoscalar interaction will be radiatively induced.

5. Comparison with β-decay constraints

We can compare our bounds on scalar currents, with those arising in nuclear β-decay. The effective Hamiltonian for allowed β-decay has the general Lorentz form [15]

$$\begin{aligned} H = \frac{G_F}{\sqrt{2}}\Big\{ & (\bar{\psi}_p\gamma_\mu\psi_n)(C_V\bar{\psi}_e\gamma_\mu\psi_\nu + C'_V\bar{\psi}_e\gamma_\mu\gamma_5\psi_\nu) \\ & + (\bar{\psi}_p\gamma_\mu\gamma_5\psi_n)(C_A\bar{\psi}_e\gamma_\mu\psi_\nu + C'_A\bar{\psi}_e\gamma_\mu\gamma_5\psi_\nu) \\ & + (\psi_p\psi_n)(C_S\bar{\psi}_e\psi_\nu + C'_S\bar{\psi}_e\gamma_5\psi_\nu) \\ & + \frac{1}{2}(\bar{\psi}_p\sigma_{\lambda\mu}\psi_n)(C_T\bar{\psi}_e\sigma_{\lambda\mu}\psi_\nu + C'_T\bar{\psi}_e\sigma_{\lambda\mu}\gamma_5\psi_\nu)\Big\}. \end{aligned} \tag{38}$$

A pseudoscalar term has not been included since it vanishes to leading order in nuclear β decay. In the absence of right-handed currents, $C_i = C'_i$ and as we have mentioned before, we consider purely scalar interactions. (Note that in the above, $\frac{1+\gamma_5}{2}$ is taken to be the left projector. This is opposite to our convention in the preceding sections. However by using this convention in this section, it will be easier to compare with the β-decay literature.) The transition probability per unit time is given by [15]

$$w_{if} = \frac{\xi}{4\pi^3}p_eE_e(E_{\max} - E_e)\left(1 + av_e\cos\theta + b\frac{2m_e}{E_e}\right)\sin\theta\,d\theta, \tag{39}$$

where $E_{\max}$ is the maximum energy of the electron in beta decay, $v_e = p_e/E_e$ and

$$\begin{aligned} \xi &= \frac{1}{2}|M_F|^2\big(|C_V|^2 + |C'_V|^2 + |C_S|^2 + |C'_S|^2\big) \\ &\quad + \frac{1}{2}|M_{GT}|^2\big(|C_A|^2 + |C'_A|^2 + |C_T|^2 + |C'_T|^2\big), \\ a\xi &= \frac{1}{2}|M_F|^2\big(|C_V|^2 + |C'_V|^2 - |C_S|^2 - |C'_S|^2\big) \\ &\quad - \frac{1}{6}|M_{GT}|^2\big(|C_A|^2 + |C'_A|^2 - |C_T|^2 - |C'_T|^2\big), \\ b\xi &= \frac{1}{2}\operatorname{Re}\big(C_SC_V^* + C'_SC'^*_V\big)|M_F|^2 + \frac{1}{2}\operatorname{Re}\big(C_TC_A^* + C'_TC'^*_A\big)|M_{GT}|^2. \end{aligned} \tag{40}$$

The angle, θ, is the angle between the electron and neutrino momenta and b is the Fierz interference term. The direct searches [2–4] for scalar interactions in β-decay consider pure Fermi transitions $0^+ \to 0^+$ as the parameter a has a particularly simple form. In this

case the Gamow–Teller matrix elements are absent and the Fermi matrix elements divide out

$$a = \frac{|C_V|^2 + |C'_V|^2 - |C_S|^2 - |C'_S|^2}{|C_V|^2 + |C'_V|^2 + |C_S|^2 + |C'_S|^2}. \tag{41}$$

Since in the standard model $C_V = C'_V = 1$, $a \neq 1$ implies evidence for an effective scalar interaction.

We need to rewrite our expressions for scalar interactions in terms of $\tilde{C}_s$ and $\tilde{C}'_s$ where $\tilde{C}_i = C_i / C_V$. The scalar couplings can be re-expressed

$$S_A = \frac{\Lambda^2 G_F \cos\theta_c}{\sqrt{2}} (\tilde{C}_s + \tilde{C}'_s), \tag{42}$$

$$S_B = \frac{\Lambda^2 G_F \cos\theta_c}{\sqrt{2}} (\tilde{C}_s - \tilde{C}'_s), \tag{43}$$

where the S_A, S_B denote scalar interactions at the nucleon level. The operator analysis of Section 3 was completed with quarks, thus we need to include the scalar form factor $\langle p|\bar{u}d|n\rangle$ which can be estimated from lattice calculations [16], $\langle p|\bar{u}d|n\rangle \approx 0.65 \pm 0.09$. By saturating the error in this quantity, we can obtain a conservative 2σ constraint equation on the scalar couplings from pion decay (see Eq. (15))

$$\begin{aligned} &-1.0 \times 10^{-2} \\ &\quad \leqslant \frac{1}{0.74} \frac{\tilde{f}_\pi \Delta_A}{f_\pi m_e} \operatorname{Re}(\tilde{C}_s + \tilde{C}'_s) + \frac{1}{0.74^2} \frac{\Delta_A^2 \tilde{f}_\pi^2}{f_\pi^2 m_e^2} |\tilde{C}_s + \tilde{C}'_s|^2 + \frac{1}{0.74^2} \frac{\Delta_B^2 \tilde{f}_\pi^2}{f_\pi^2 m_e^2} |\tilde{C}_s - \tilde{C}'_s|^2 \\ &\quad \leqslant 2.2 \times 10^{-3}. \end{aligned} \tag{44}$$

If we include only left-handed neutrinos in the theory, we are constrained to lie along the line $\tilde{C}_s = \tilde{C}'_s$ whereas if we include only right-handed neutrinos we are forced to lie along $\tilde{C}_s = -\tilde{C}'_s$. We can now examine a few special cases.

In the absence of right-handed neutrinos, if we consider C_s and C'_s to be purely real and the scale Λ of the order of 200 GeV, the indirect limits from $\pi^\pm \to l^\pm \nu_l$ decay give us the limit

$$-1.2 \times 10^{-3} \leqslant \tilde{C}_s \leqslant 2.7 \times 10^{-4}. \tag{45}$$

For comparison, the experimental 90% confidence limit determined from the b-Fierz interference term in β-decay (see Eq. (40)) is $|\operatorname{Re}(\tilde{C}_s)| \leqslant 8 \times 10^{-3}$ [3,5]. We see that the indirect limit from pion decay is stronger by over an order of magnitude. On the other hand, if we consider C_s and C'_s to be purely imaginary; again in the limit of left-handed couplings we obtain

$$|\tilde{C}_s| \leqslant 1.2 \times 10^{-2} \tag{46}$$

where the scale Λ is of the order of 200 GeV. Again for comparison, the experimental limit on the size of the imaginary part at the 95% confidence level, with only left-handed neutrinos, is approximately $|\operatorname{Im}(\tilde{C}_s)| \leqslant 1 \times 10^{-1}$ [3]. The indirect $\pi^\pm \to l^\pm \nu_l$ limit is stronger by approximately an order of magnitude. If we take $\tilde{C}_s = -\tilde{C}'_s$ so that we are in

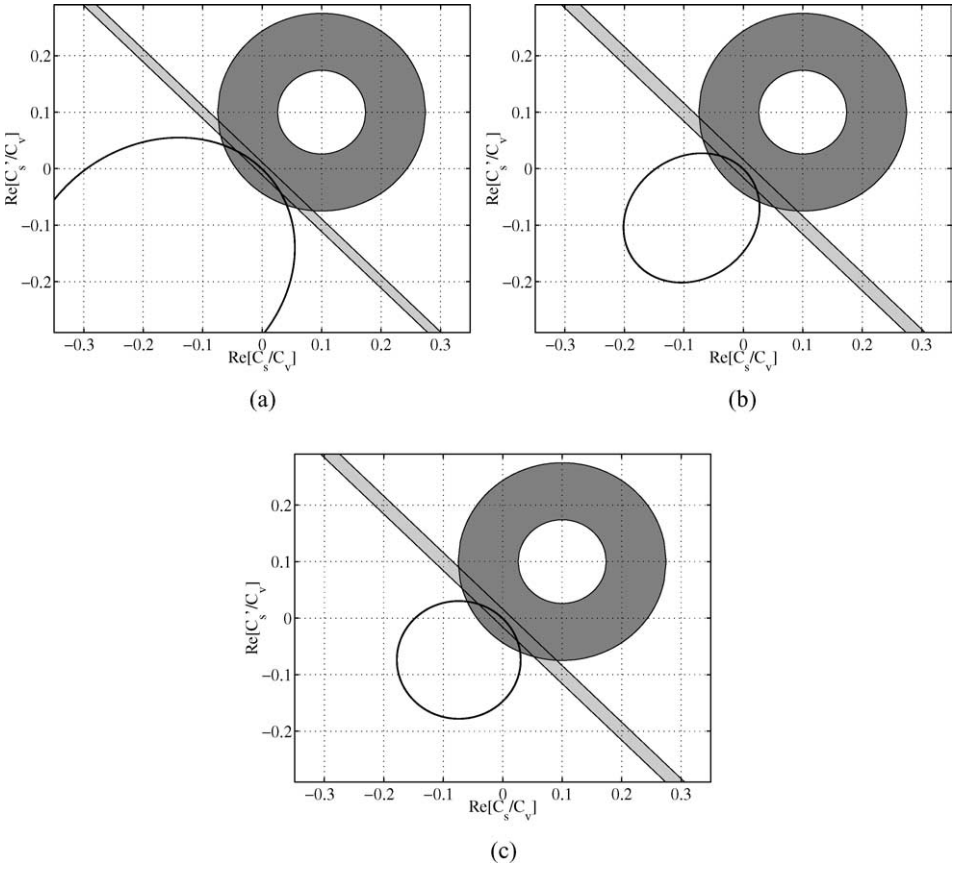

Fig. 10. Constraint plots on the real parts of $\tilde{C}_S$ and $\tilde{C}'_S$ at $\Lambda = 200$ GeV. Panel (a) corresponds to a phase of $0°$; panel (b) to $\pm 45°$; and panel (c) to $45°$ and $-45°$ for $\tilde{C}_S$ and $\tilde{C}'_S$, respectively. The diagonal band is the experimental limit set by the b-Fierz interference term from β-decay at the 90% confidence level and the solid annulus is the approximate experimental bound given in [3]. In all cases, the allowed region is the band between the two ellipses. An enlargement of the figures is displayed in Fig. 11.

the limit of right-handed couplings and the b-Fierz interference term vanishes we find

$$|\tilde{C}_S| \leqslant 1.0 \times 10^{-2}. \tag{47}$$

Again for comparison, at 1σ, the direct experimental constraint is $|\tilde{C}_S| \leqslant 6 \times 10^{-2}$ [3]. In each case presented the scale of new physics was at $\Lambda = 200$ GeV corresponding to $\Delta_A(200\ \text{GeV}) \approx 7.7 \times 10^{-4}$, $\Delta_B(200\ \text{GeV}) \approx 8.9 \times 10^{-4}$. Because the pseudoscalar interactions are induced through renormalization group running from Λ down to the electroweak scale, the higher the scale of new physics is, the more competitive our results become relative to beta decay. As the scale of new physics is lowered, the constraints from $\pi^{\pm} \to l^{\pm}\nu_l$ become less stringent. However even in the worst case limit where the new scale is at the Z-mass and therefore we would no longer have an interval of renormalization group running, the renormalization threshold effects calculated in Eq. (36) are

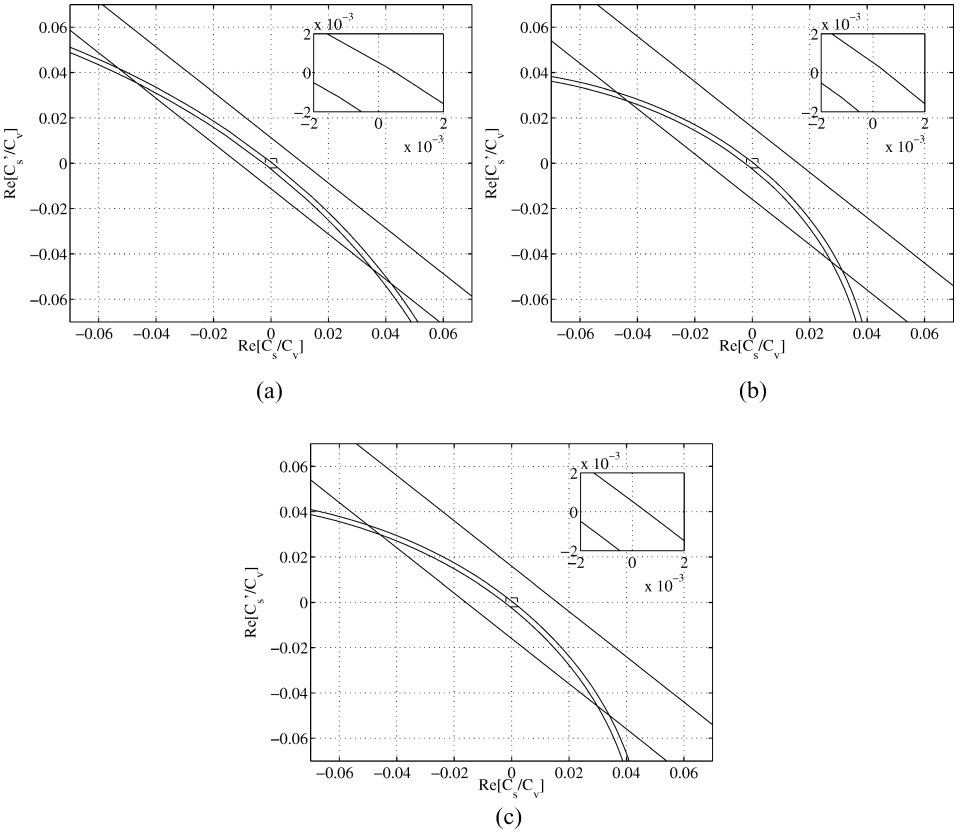

Fig. 11. Constraint plots on the real parts of $\tilde{C}_S$ and $\tilde{C}'_S$ at $\Lambda = 200$ GeV. Panel (a) corresponds to a phase of 0°; panel (b) to ±45°; and panel (c) to 45° and −45° for $\tilde{C}_S$ and $\tilde{C}'_S$, respectively. The diagonal band is the experimental limit set by the b-Fierz interference term from β-decay at the 90% confidence level. In all cases, the allowed region is the band between the two ellipses. The enlarged area more clearly shows the width of the region.

still competitive. As an example, if we take C_S and C'_S to be real and ignore right-handed neutrinos we find that

$$-2 \times 10^{-2} \leqslant \tilde{C}_S \leqslant 4 \times 10^{-3}. \tag{48}$$

Plots of the pion physics constraints for the more general situation (where the real and imaginary parts of C_S and C'_S vary independently) are given in Figs. 10–13. We plot the constraints for the real and imaginary parts separately. Note from Eq. (44) that the phases of C_S and C'_S are important when constructing these separate plots. In order to convey the effects of the phases most clearly, we have chosen three interesting cases. In the real plots we consider: C_S and C'_S to each have a phase of 0°; C_S and C'_S to each have a phase of ±45°; and the situation where C_S has as a phase of 45° and C'_S has a phase of −45°. In the imaginary plots we consider: C_S and C'_S to each have a phase of ±90°; C_S and C'_S each have a phase of ±45°; and the case where C_S has a phase of 45° and C'_S has a phase of

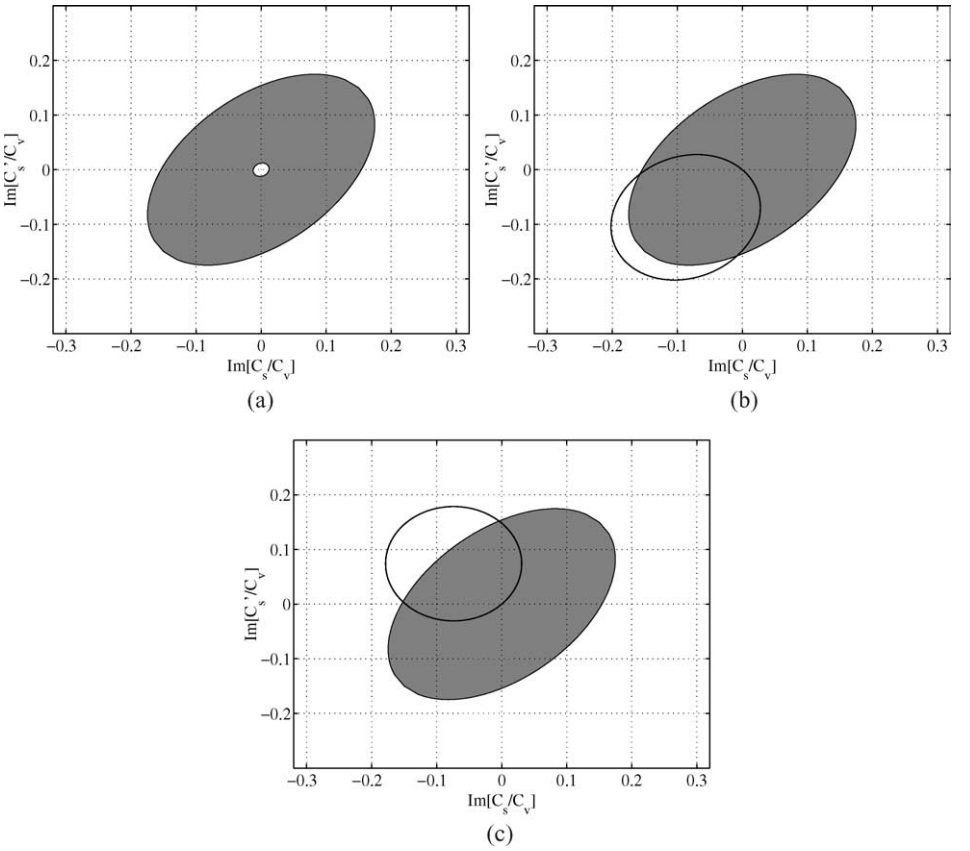

Fig. 12. Constraint plots on the imaginary parts of $\tilde{C}_S$ and $\tilde{C}'_S$ at $\Lambda = 200$ GeV. Panel (a) corresponds to a phase of $\pm 90°$; panel (b) to $\pm 45°$; and panel (c) to $45°$ and $-45°$ for $\tilde{C}_S$ and $\tilde{C}'_S$, respectively. The solid ellipse is the approximate experimental bound on the imaginary part of the couplings assuming nothing about the phase [3]. In panel (a), the unshaded interior ellipse is the constraint from pion decay. In the remaining plots, the allowed region is the band between the two ellipses. An enlargement of the figures is displayed in Fig. 13.

$-45°$. All three plots in the imaginary case are well within the region allowed by the direct experimental bounds [3,17].

There are two points of interest that warrant further discussion. First, note that in the limit of sufficiently large phases (i.e., $> 85°$) the ellipse bound in Fig. 11 moves entirely inside the b-Fierz interference limit allowed region. This is expected since phases approaching $90°$ imply that C_S and C'_S are almost completely imaginary. When this situation occurs and we are in the limit of left-handed couplings (i.e., along the line $C_S = C'_S$), there are two solutions consistent with the pion physics constraints and the b-Fierz interference bound. One solution is centered around 0 and the other is centered off 0 along the line $C_S = C'_S$ yet inside the b-Fierz interference limits. Even in these cases, the width of the ellipse bound is still of the order of 2×10^{-3}. Secondly, in order to move from the origin along the ellipse by more than the width of the allowed region requires a delicate cancel-

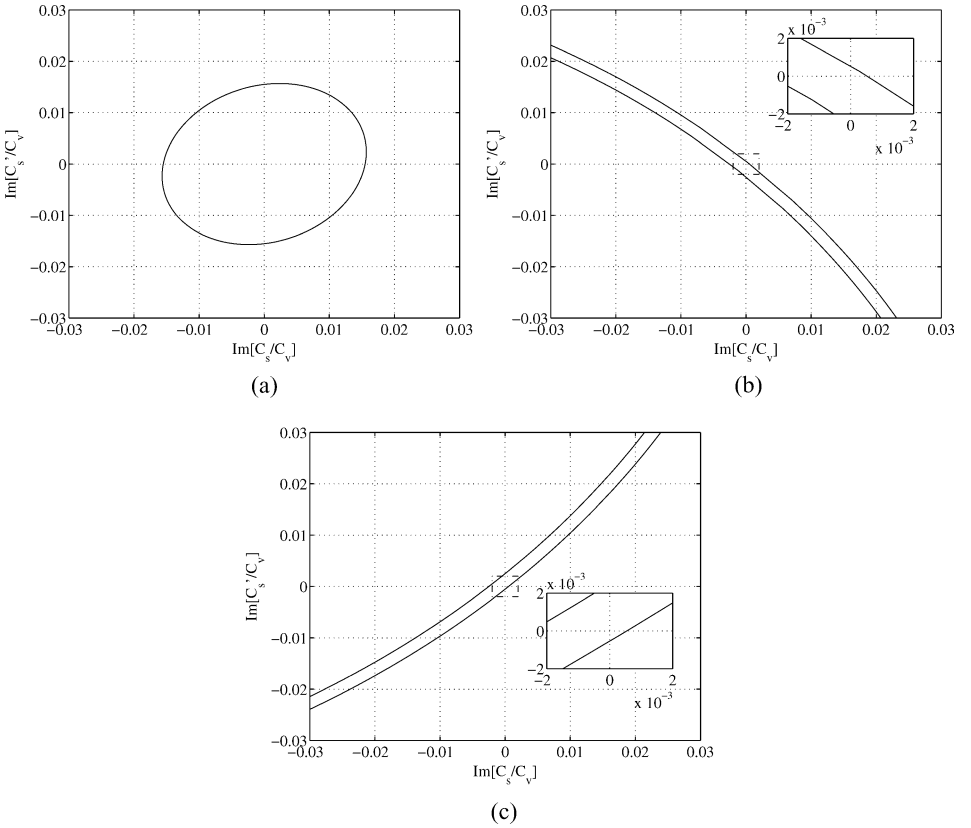

Fig. 13. Constraint plots on the imaginary parts of $\tilde{C}_S$ and $\tilde{C}'_S$ at $\Lambda = 200$ GeV. Panel (a) corresponds to a phase of $\pm 90°$; panel (b) to $\pm 45°$; and panel (c) to $45°$ and $-45°$ for $\tilde{C}_S$ and $\tilde{C}'_S$, respectively. In panel (a), the interior of the ellipse is the constraint. In the remaining plots, the allowed region is the band between the two ellipses. The enlarged area more clearly shows the width of the region.

lation between the terms in Eq. (44). If we ignore the possibility of this cancellation, the region allowed by pion decay would collapse to a small region near the origin of length given by the width of the ellipse bounds.

6. Flavour dependent couplings

Thus far we have obtained limits on scalar interactions in the limit of universal flavour couplings. Let us now relax this assumption. One case that deserves attention is the limit of mass proportional couplings. This implies that $R_e/(m_e^2(m_\pi^2 - m_e^2)) = R_\mu/(m_\mu^2(m_\pi^2 - m_\mu^2))$ in Eq. (10) and therefore there is no effect on the pion branching ratio

$$\frac{\Gamma(\pi^- \to e\nu_e)}{\Gamma(\pi^- \to \mu\nu_\mu)} = \frac{(m_\pi^2 - m_e^2)}{(m_\pi^2 - m_\mu^2)}\left[\frac{m_e^2(m_\pi^2 - m_e^2) + S_e}{m_\mu^2(m_\pi^2 - m_\mu^2) + S_\mu}\right] = T. \tag{49}$$

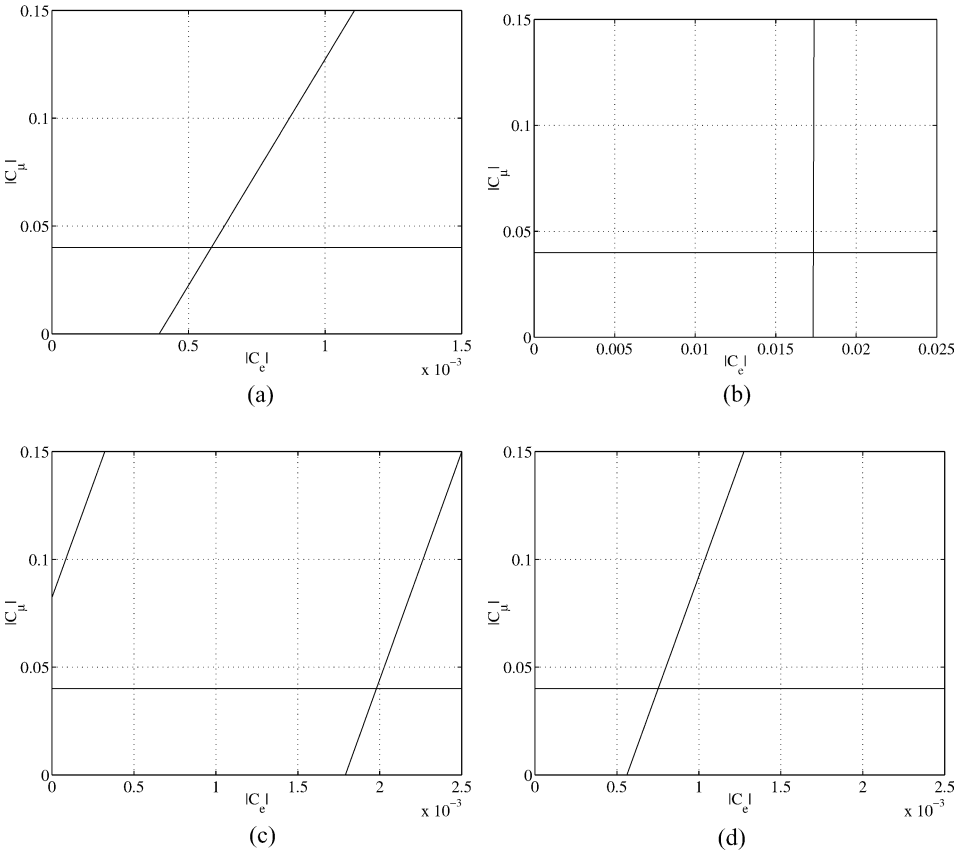

Fig. 14. Constraint plots on the $|C_e|$ and $|C_\mu|$ couplings at $\Lambda = 200$ GeV. Panel (a) corresponds to phases for C_e and C_μ of 0°, 0°; panel (b) to 90°, 90°; panel (c) to 180°, 180°; panel (d) to ±45°, ±45°, respectively. The allowed region is the bounded area in the lower left corner. The horizontal line is the muon capture bound [18].

This observation also holds in the presence of right-handed neutrinos. However, in this case, we still can bound the scalar couplings involved in β-decay by combining the $\pi^\pm \to l^\pm \nu_l$ limits with data from muon capture experiments. Recent experiments and analysis of muon capture on ^{3}He indicate that the muon–nucleon scalar coupling is bounded by [18]

$$\frac{|S_\mu|}{\Lambda^2} \leqslant 4 \times 10^{-2} G_F \tag{50}$$

with a neutrino of left-handed chirality. Therefore, in the limit of mass proportional couplings, S_e/Λ^2 must be of the order of 200 times smaller due to the electron–muon mass ratio. This implies that $\tilde{C}_s$ is bounded

$$|\tilde{C}_s| \leqslant 2 \times 10^{-4}. \tag{51}$$

In order to estimate the degree to which the presence of muon scalar interactions can weaken the limits that we infer from $\pi^\pm \to l^\pm \nu_l$, let us assume that the muon scalar coupling saturates the experimental bound Eq. (50). Substituting this into the expression for

the pion branching ratio Eq. (13), ignoring right-handed neutrinos and assuming a scale Λ of 200 GeV, Eq. (15) is modified to the following form:

$$-3.3\times10^{-2}\leqslant\sqrt{2}\frac{\tilde{f}_\pi\,\mathrm{Re}(\rho)}{G_F\Lambda^2 f_\pi\cos\theta_c m_e}+\frac{|\rho|^2\tilde{f}_\pi^2}{2G_F^2\Lambda^4 f_\pi^2\cos^2\theta_c m_e^2}\leqslant 7.3\times10^{-3}. \quad (52)$$

We find this conservative approach has the effect of weakening our limits a factor of three at most compared to the analysis in Section 5. The limits on scalar couplings with $\Lambda=$ 200 GeV, from $\pi^\pm\to l^\pm\nu_l$ combined with muon capture scalar limits, are substantially stronger than limits on scalar couplings from direct β-decay searches.

Finally, we consider the allowed region for the electron-scalar and muon-scalar couplings in a model independent manner. Again the constraint equation derived from Eq. (13) is

$$-1.0\times10^{-2}\leqslant\left(\frac{1+\sqrt{2}\frac{\tilde{f}_\pi\,\mathrm{Re}(C_e)\Delta_A}{f_\pi\cos\theta_c m_e}+\frac{|C_e|^2\Delta_A^2\tilde{f}_\pi^2}{2f_\pi^2\cos^2\theta_c m_e^2}}{1+\sqrt{2}\frac{\tilde{f}_\pi\,\mathrm{Re}(C_\mu)\Delta_A}{f_\pi\cos\theta_c m_\mu}+\frac{|C_\mu|^2\Delta_A^2\tilde{f}_\pi^2}{2f_\pi^2\cos^2\theta_c m_\mu^2}}-1\right)\leqslant 2.2\times10^{-3}, \quad (53)$$

where

$$C_\mu=\frac{S_\mu}{G_F\Lambda^2},\qquad C_e=\frac{S_e}{G_F\Lambda^2}. \quad (54)$$

We display the results in Fig. 14 for a number of different phase conditions. We consider the cases where the complex phase of C_e and C_μ are 0°, 0°; 90°, 90°; 180°, 180°; ±45°, ±45°, respectively.

7. Discussion

By considering renormalization effects on universal (or alternatively first generation), and flavour diagonal scalar operators, we have derived limits on the size of the ratio between scalar and vector couplings from precision measurements of $\pi^\pm\to l^\pm\nu_l$ decay. As a typical constraint value, in the absence right-handed neutrinos, we find that $-1.2\times10^{-3}\leqslant\tilde{C}_s\leqslant 2.7\times10^{-4}$ for Λ of the order of 200 GeV. A more general comparison with the β-decay experiments (with the inclusion of right-handed neutrinos) is made in the plots in Figs. 11 and 13. We note that the most conservative estimate of the limits occurs when the new physics arises at the electroweak scale. In this case, the contribution to the induced pseudoscalar comes entirely from threshold corrections which we estimate from the calculations in Section 4. The limit for real couplings in the absence of right-handed neutrinos from threshold contributions is $-3\times10^{-2}\leqslant\tilde{C}_s\leqslant 6\times10^{-3}$. In the scenario where we have arbitrary generation dependence of the scalar couplings, $\pi^\pm\to l^\pm\nu_l$ limits can be combined with limits on scalar interactions in muon capture to bound the first generation scalar couplings. These limits are illustrated in particular cases in Fig. 14.

These observations have implications for current β-decay experiments. Direct searches for scalar interactions in β-decay will be most competitive if the new physics responsible for the effective scalar interactions arises at the electroweak scale in the explicit exchange of new scalar particles. In these circumstances, the indirect limits from threshold induced

pseudoscalar interactions, Eq. (48), are comparable to the direct β-decay scalar searches. Therefore, interest in searches for new scalar interactions with β-decay experiments remains undiminished.

On the other hand, for new effective scalar interactions arising as effective $SU(2) \times U(1)$ invariant operators at mass scales above 200 GeV (as expected in models with leptoquarks, composite quarks/leptons, or low scale quantum gravity) the constraints arising from the precision measurements of $\pi^{\pm} \to l^{\pm}\nu_l$ decay, combined with limits on scalar interactions in muon capture, can be stronger by an order of magnitude or more than the direct experimental searches. Furthermore, the relative strength of these searches becomes better, the higher the mass scale of the new physics compared to the electroweak scale. This argues strongly for improved experimental precision in measurements of muon capture, and $\pi^{\pm} \to l^{\pm}\nu_l$ decay. In particular we note that in the case of pion decay, the experimental error exceeds the uncertainty in the theoretical calculation by a factor of eight. A new measurement of $\pi^{\pm} \to l^{\pm}\nu_l$ decay with an order of magnitude greater precision would not only constrain physics beyond the standard model which could potentially contribute to tree level pion decay, but as we have argued above, will also indirectly provide tests of new scalar interactions of unparalleled precision.

Acknowledgements

We would like to thank Eric Adelberger and John Behr for their generous assistance at several stages of this project. We are especially grateful for the help that John Behr and Manuella Vincter extended to us in regards to issues in error analysis. We have benefited from useful discussions with Doug Bryman, Andrzej Czarnecki, John Ellis, Randy Lewis, Michael Luke, and Aneesh Manohar. We wish to thank J.P. Archambault, Eric Carpenter and David Shaw for their help with the Feynmf package and graphics. This work was supported by the Natural Sciences and Engineering Research Council of Canada.

References

[1] Particle Data Group, Phys. Rev. D 66 (2002).
[2] A. Garcia, et al., nucl-ex/9904001.
[3] ISOLDE Collaboration, E.G. Adelberger, et al., Phys. Rev. Lett. 83 (1999) 1299, nucl-ex/9903002.
[4] E.G. Adelberger, Phys. Rev. Lett. 70 (1993) 2856.
[5] For a review see: I.S. Towner, J.C. Hardy, nucl-th/9504015.
[6] For a review see: D.A. Bryman, Comments Nucl. Part. Phys. 21 (1993) 101.
[7] W.J. Marciano, A. Sirlin, Phys. Rev. Lett. 71 (1993) 3629.
[8] D.I. Britton, et al., Phys. Rev. Lett. 68 (1992) 3000–3003.
[9] D.I. Britton, et al., Phys. Rev. D 49 (1993) 17–20.
[10] D.I. Britton, et al., Phys. Rev. Lett. 70 (1992) 3000–3003.
[11] For review see: A. Manohar, hep-ph/9606222;
For review see: D. Kaplan, nucl-th/9506035.
[12] S. Weinberg, Physica A 96 (1979) 327–340.
[13] H. Arason, D.J. Castano, B. Keszthelyi, S. Mikaelian, E.J. Piard, P. Ramond, B.D. Wright, Phys. Rev. D 46 (1992) 3945–3965.
[14] B.D. Wright, hep-ph/9404217.

[15] J. Jackson, S. Treiman, H. Wyld Jr., Nucl. Phys. 4 (1957) 206.
[16] S.J. Dong, J.F. Lagaë, K.F. Liu, Phys. Rev. D 54 (1996) 5496–5500, hep-ph/9602259.
[17] M.B. Schneider, et al., Phys. Rev. Lett. 51 (1983) 1239.
[18] J. Govaerts, J.-L. Lucio-Martinez, Nucl. Phys. A 678 (2000) 110, nucl-th/0004056.